

Model of P- and T-Electroreceptors of Weakly Electric Fish

Yoshiki Kashimori, Mituyuki Goto, and Takeshi Kambara

Department of Applied Physics and Chemistry, The University of Electro-Communications, Chofu, Tokyo 182, Japan

ABSTRACT To clarify the microscopic mechanisms by which P- and T-receptors encode amplitude modulation and zero crossing time of jamming signals, we present a model of P- and T-receptors based on their physiological and anatomical properties. The model consists of a receptor cell, supporting cells, and an afferent nerve fiber. The basal membrane of the receptor cell includes voltage-sensitive Ca^{2+} channels, Ca^{2+} -activated K^+ channels, and leak channels of Na^+ , K^+ , and Cl^- . The driving force of potential change under stimulation is generated by the voltage-sensitive Ca^{2+} channels, and the suppressing force of the change is generated by Ca^{2+} -activated K^+ channels. It has been shown that in T-receptor cells the driving force is much stronger than the suppressing force, whereas in P-receptor cells the driving force is comparable with the suppressing force. The differences in various kinds of response properties between P- and T-receptors have been consistently explained based on the difference in the relative strengths of the driving and suppressing forces between P- and T-receptor cells. The response properties considered are encoding function, probability of firing of afferent nerve, pattern of damped oscillation, shape of tuning curves, values of the optimum frequency, and response latency.

INTRODUCTION

Weakly electric fish perceive objects in their environment by detecting distortions of their electric organ discharge (EOD) field (Bastian, 1986). When detection is jammed by interference between their own EODs and those of their neighbors, the fish shifts the frequency of its own EOD away from those of its neighbor's EOD to avoid the jam. The neural basis of the jamming avoidance response in the gymnotiform wave species *Eigenmannia* has been studied in great detail from receptors to spinal motor neurons (Heiligenberg, 1991).

Eigenmannia makes use of the modulation of EOD amplitude and phase to overcome interference. In the initial stage of the jamming avoidance response, two kinds of modulation are coded by two kinds of receptors, P-receptors and T-receptors (Zakon, 1986a), which code modulations of EOD amplitude and EOD phase, respectively. T-receptors fire at the rate of one spike per EOD cycle, that is, they are phase-locked to the EOD. Therefore, T-receptors can generate signals that contain information with respect to the time of positive zero crossing in the EOD wave, that is, they code the phase of the EOD. On the other hand, P-receptors fire with a probability of less than 1.0 for stimuli within the normal EOD intensity range. Because the firing probability changes with stimulus intensity, the amplitude of EOD can be coded by P-receptors.

In the present paper, we are concerned with the microscopic mechanism of encoding of the two kinds of receptors, T-receptors and P-receptors. To better understand the

mechanism, many workers have studied various kinds of response properties of receptors (Bastian, 1994; Bennett and Obara, 1986; Zakon, 1986a). Bennett (1967) proposed an equivalent circuit model of the receptors that consisted of high-pass and low-pass filters. Scheich et al. (1973) extended the model to reproduce the dependence of sensitivity on stimulus frequency (tuning curve) for the P- and T-receptors. However, the molecular origins of the low-pass and the high-pass filters have not been described. Therefore, we can apply phenomenological models to the study of tuning, but not to many other properties.

To systematically clarify the microscopic origins of most of the observed fundamental properties of P- and T-receptors, we present a microscopic model of the P- and T-receptors based on the physiological and anatomical results observed for these receptors (Zakon, 1986a). The receptor systems considered consist of a receptor cell, a tight junction made by supporting cells, and an afferent nerve fiber innervating the receptor cell, as shown in Fig. 1. The apical membrane includes only leak channels of Na^+ , K^+ , and Cl^- (Bennet and Obara, 1986). The basal membrane includes voltage-sensitive Ca^{2+} channels and Ca^{2+} -activated K^+ channels, in addition to leak channels for Na^+ , K^+ , and Cl^- .

We show, based on the calculated results for various kinds of response properties of P- and T-receptors, that the functional difference between P- and T-receptors comes essentially from the difference in relative strength of contributions of the Ca^{2+} channels and the K^+ channels to the response property of receptor cells between the two receptors. The driving force of potential change under stimulation is generated by Ca^{2+} channels, whereas the suppressing force of the changes is generated by K^+ channels. In the T-receptor cells, the driving force is much stronger than the suppressing force, but in the P-receptor cells, the driving force is comparable to the suppressing force.

Received for publication 13 September 1995 and in final form 28 February 1996.

Address reprint requests to Dr. Yoshiki Kashimori, Department of Applied Physics and Chemistry, University of Electrocommunications, Chofu, Tokyo 182, Japan. Tel.: 81-424-832161; Fax: 81-424-89-9748; E-mail: kashi@nerve.pc.vec.ac.jp.

© 1996 by the Biophysical Society

0006-3495/96/06/2513/14 \$2.00

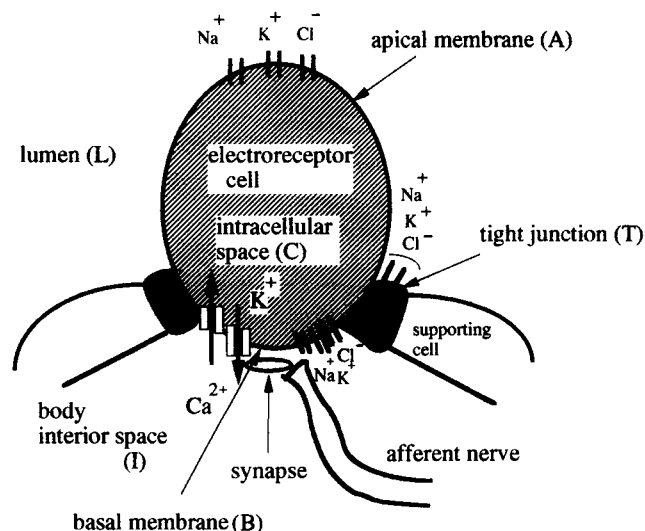


FIGURE 1 Schematic representation of a tuberosus electroreceptor of weakly electric fish. Tight junctions seal off the extracellular space (body interior) between the receptor and supporting cells, and divide the receptor cell membrane into apical and basal membranes. Leak channels of Na^+ , K^+ , and Cl^- exist in the apical and basal membranes and in the tight junctions. Besides the leak channels, the basal membrane has voltage-sensitive Ca^{2+} channels and Ca^{2+} -activated K^+ channels.

The threshold intensity of sinusoidal stimulation for the firing of T-receptors at the rate of one spike per stimulation cycle depends on the frequency of the stimulation. The dependences show a V-shaped curve (Hopkins, 1976; Viancour, 1979a). The afferent fiber becomes most sensitive to frequency (called the optimum frequency) at the minimum point. It has been shown (Keller et al., 1986; Meyer et al., 1984; Zakon, 1986b) that the optimum frequencies of individual T-receptors are in close correlation with the frequencies of damped oscillatory responses of the receptor cells (called receptor oscillation) induced by brief stimulation with an electric pulse. Although the sharp tuning of receptor sensitivity has been suggested to be determined by active ion conductances (Bennett, 1967; Hopkins, 1976; Viancour, 1979a; Zakon, 1984, 1986b; Zakon and Meyer, 1983), the microscopic mechanism by which the optimum frequencies are determined has not yet been clarified.

Using the microscopic model of receptor systems, we determine quantitatively as well as qualitatively the frequency and number of cycles of underdamped receptor oscillations. That is, the patterns of oscillation are predictable and the frequency sensitivities of P- and T-receptors correlate with the properties of the receptor oscillation. The frequency and number of oscillation cycles increase as the driving force of potential change, that is, population density and/or ionic conductance of Ca^{2+} channels increases. Conversely, as the suppressing force, that is, density and/or conductance of Ca^{2+} -activated K^+ channels increases, the frequency is increased, but the number of oscillation cycles is decreased. When the frequency of the sinusoidal stimulus is set to the resonant frequency of the receptor oscillation, the afferent nerve becomes most sensitive to the stimulus.

MODEL

A model of the electroreceptor cell system

We present a model of the receptor system in tuberosus receptor organs of weakly electric fish. The model is shown schematically in Fig. 1. The receptor system consists of a receptor cell, supporting cells, and an afferent nerve fiber. The three kinds of solution regions are lumen, intracellular spaces, and body interior space. Because we consider the variation in potential across the basal membrane of the receptor cell, which is induced by electric stimulation applied to the lumen, we take into account the ionic currents only across the apical and basal membranes of the receptor cell and the tight junction between the receptor and supporting cells.

We consider the leak channels of Na^+ , K^+ , and Cl^- to be included in the apical and basal membranes and the tight junction. The leak channels contribute mainly to the determination of resting potential of the receptor cell. It is likely (Bennett and Obara, 1986; Zakon, 1984) that the receptor cells have voltage-sensitive Ca^{2+} channels and Ca^{2+} -activated K^+ channels that are responsible for their regenerative voltage responses. The apical membrane does not include active channels (Bennet and Obara, 1986). Therefore, the present model has voltage-sensitive Ca^{2+} channels and Ca^{2+} -activated K^+ channels in the basal membrane.

Impulse generation in the afferent nerve fiber is induced by transmitter release, which occurs when the basal membrane potential is depolarized.

Equations for the potentials across the apical and basal membranes

We describe the equations by which variations of the electric potentials ϕ_A and ϕ_B across the apical and basal membranes, respectively, are determined under external electric stimulus. To derive the equations, we use an equivalent circuit model shown in Fig. 2 for the receptor cell system.

We obtain the equations from the conservation laws of the electric current densities I_A , I_B , and I_T , which are flowing across the apical membrane (A), the basal membrane (B), and the tight junction (T), respectively,

$$S_A I_A + S_T I_T = -(S_A + S_T) I_{\text{stim}}, \quad (1)$$

$$S_A I_A = -S_B I_B, \quad (2)$$

where I_X is the current density across a unit area of the membrane X ($X = A, B, T$), S_X is the area of membrane X, and I_{stim} is a stimulation current applied to the system.

Each current consists of ionic flows through ion channels and displacement current and is written as

$$I_A = C_A \frac{d\phi_A}{dt} + \sum_{\nu} f_{\nu}^A (\phi_A - \phi_{\nu}^A), \quad (3)$$

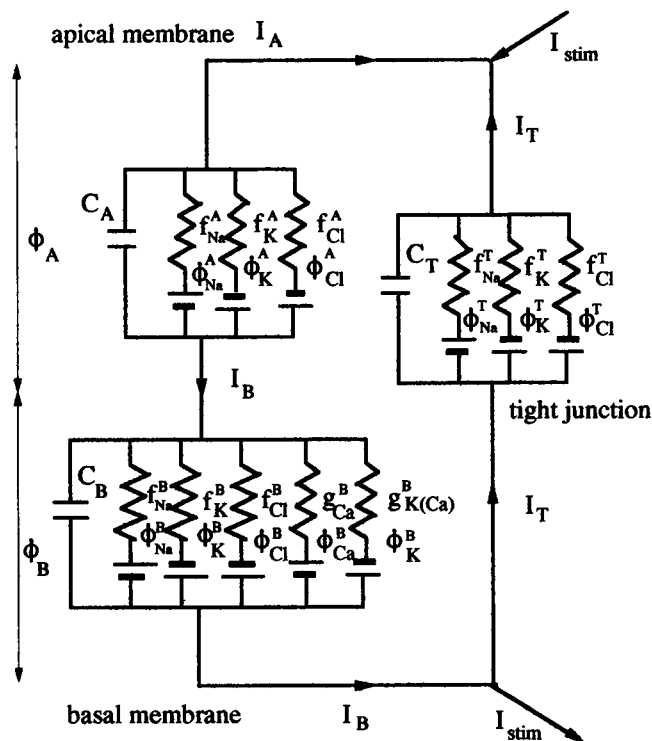


FIGURE 2 The equivalent circuit of the receptor model. g_{ν}^B ($\nu = \text{Ca}$, $\text{K}(\text{Ca})$) mean conductance of ion channel ν in the basal membrane, f_{ν}^X ($\nu = \text{Na}^+$, K^+ , Cl^- ; $X = \text{A}$, B , T) the conductance of leak channel of ν in the membrane X , and ϕ_{ν}^X the equilibrium potentials of ion ν across the membrane X . C_X is the capacitance of the membrane X . I_X denotes the current density across the membrane X . The arrows attached to I_{stim} and I_X indicate the positive directions of relevant current.

$$I_B = C_B \frac{d\phi_B}{dt} + \sum_{\nu} f_{\nu}^B (\phi_B - \phi_{\nu}^B) + g_{\text{Ca}}^B (\phi_B - \phi_{\text{Ca}}^B) + g_{\text{K}(\text{Ca})}^B (\phi_B - \phi_{\text{K}}^B), \quad (4)$$

$$I_T = C_T \frac{d\phi_T}{dt} + \sum_{\nu} f_{\nu}^T (\phi_T - \phi_{\nu}^T), \quad (5)$$

where C_X ($X = \text{A}$, B , T) is the capacitance of a unit area of membrane X ; f_{ν}^X ($\nu = \text{Na}^+$, K^+ , Cl^-) is the electric conductance of the leak channels of ion ν in a unit area of the membrane X ; g_{Ca}^B and $g_{\text{K}(\text{Ca})}^B$ are the conductances of voltage-sensitive Ca^{2+} channels and Ca^{2+} -activated K^+ channels in a unit area of basal membrane, respectively, and ϕ_{ν}^X is the equilibrium potential of ion ν across the membrane X . The potential ϕ_{ν}^X is given by

$$\phi_{\nu}^X = \frac{RT}{z_{\nu} F} \ln [C_{\nu}^Y / C_{\nu}^Z], \quad (6)$$

where X , Y , and Z stand for a membrane and two solution regions across the membrane, respectively; (X, Y, Z) takes $(\text{A}, \text{L}, \text{C})$, $(\text{B}, \text{I}, \text{C})$, and $(\text{T}, \text{L}, \text{I})$; ν stands for Na^+ , K^+ , Cl^-

and Ca^{2+} ; C_{ν}^Y means the concentration of ion ν in the region Y ; z_{ν} is the valency of ion ν ; and F , R , and T have their usual meanings. The potential of the tight junction, ϕ_T , is represented as a function of ϕ_A and ϕ_B ,

$$\phi_T = \phi_A - \phi_B. \quad (7)$$

The equations for ϕ_A and ϕ_B are obtained by substituting Eqs. 3–5 and 7 in Eqs. 1 and 2 as

$$\frac{d\phi_A}{dt} = \frac{1}{CR_{\text{AT}}} \{ -(r_A + r_T) I_{\text{stim}} - r_A (1 + r_T) G_A - r_T G_B - r_T G_T \}, \quad (8)$$

$$\frac{d\phi_B}{dt} = \frac{1}{CR_{\text{AT}}} \{ r_A (r_A + r_T) I_{\text{stim}} - r_A r_T G_A - (r_A + r_T) G_B + r_A r_T G_T \}, \quad (9)$$

where

$$G_A \equiv \sum_{\nu} f_{\nu}^A (\phi_A - \phi_{\nu}^A), \quad (10)$$

$$G_B \equiv \sum_{\nu} f_{\nu}^B (\phi_B - \phi_{\nu}^B) + g_{\text{Ca}}^B (\phi_B - \phi_{\text{Ca}}^B) + g_{\text{K}(\text{Ca})}^B (\phi_B - \phi_{\text{K}}^B), \quad (11)$$

$$G_T \equiv \sum_{\nu} f_{\nu}^T (\phi_A - \phi_B - \phi_{\nu}^T), \quad (12)$$

$$R_{\text{AT}} \equiv r_A + r_T + r_T r_A, \quad r_A \equiv S_A / S_B, \quad r_T \equiv S_T / S_B, \quad (13)$$

and the summation over ν is taken for Na^+ , K^+ , and Cl^- . Here, for simplicity, we present expressions only for the case where $C_A = C_B = C_T (= C)$.

To calculate the values of ϕ_A and ϕ_B for various stimulation currents I_{stim} , we need to represent the conductivities f_{ν}^X , g_{Ca}^B , and $g_{\text{K}(\text{Ca})}^B$ of ionic channels considered as functions of membrane potentials ϕ_A and ϕ_B and of the concentrations of relevant ions in the three kinds of solution regions L, C, and I. We describe the conductivities of leak channels f_{ν}^X using Goldman's approximation for the Nernst-Planck ion flux equation (Lakshminarayanaiah, 1984). They are given by

$$f_{\nu}^X = \frac{z_{\nu}^2 F^2 \phi_X P_{\nu}^X}{RT (\phi_X - \phi_{\nu}^X)} \frac{C_{\nu}^Y - C_{\nu}^Z \exp(z_{\nu} \theta_X)}{1 - \exp(z_{\nu} \theta_X)}, \quad (14)$$

where the meanings of X , Y , and Z are the same as those in Eq. 6; ν stands for ions Na^+ , K^+ , and Cl^- ; $\theta_X = F \phi_X / RT$, and P_{ν}^X is the permeability of ion ν across the membrane X .

For the conductivity g_{Ca}^B of the Ca^{2+} channels and $g_{\text{K}(\text{Ca})}^B$ of the Ca^{2+} -activated K^+ channels, we use the mathematical expressions of the channels given in the model of a hair cell presented by Hudspeth and Lewis (1988a, b). The hair cell has a sharply tuned sensitivity to stimulus frequency, as

the T-receptor does. In another analogy to hair cells, voltage-sensitive Ca^{2+} channels and Ca^{2+} -activated K^+ channels have been suggested (Bastian, 1994; Zakon, 1984, 1986a, b) to play an important role in the response of the receptor. Because we adjust the values of some parameters in the expressions so as to reproduce the observed value of tuning frequency for receptors, the mathematical expressions of the channels are briefly summarized in the Appendix.

Description of response of afferent nerve fiber

To calculate the impulse trains on the afferent nerve fiber induced by depolarization of the receptor cell, we use the Hodgkin-Huxley equations (Hodgkin and Huxley, 1952). Each spike in the postsynaptic axon terminal of the afferent nerve innervating the receptor cells has been shown (Murray and Capranica, 1973; Pabst, 1977; Sanchez and Zakon, 1990) to be initiated at the base of each receptor organ.

The membrane potential V at the axon terminal is determined by

$$C_N \frac{dV}{dt} = -\bar{g}_{\text{Na}} m^3 h (V - V_{\text{Na}}) - \bar{g}_{\text{K}} n^4 (V - V_{\text{K}}) - g_{\text{L}} (V - V_{\text{L}}) + I_{\text{ps}}, \quad (15)$$

where C_N is the capacitance of the axon membrane; \bar{g}_{Na} and \bar{g}_{K} are the maximum conductances of the active Na^+ and K^+ channels, respectively, when all channels are opened; g_{L} is the conductance of leak channel (Cl^- channel); m , h , and n are the gating parameters; and V_{ν} is the equilibrium potential of ion ν ($\nu = \text{Na}^+, \text{K}^+, \text{Cl}^-$). The gating parameters are determined by the linear rate equations, the explicit description of which appears in the Appendix, because we change slightly the parameter values given by Hodgkin and Huxley (1952).

The postsynaptic current I_{ps} in Eq. 15 is induced by the neural transmitter released from the presynaptic membrane of the receptor cell. The magnitude of I_{ps} is nearly proportional to the amount of released transmitter, which is determined by the Ca^{2+} current I_{Ca}^{B} across the basal membrane. Because it seems reasonable that the amount is proportional to a sigmoid function of I_{Ca}^{B} , we represent the relation of I_{ps} to I_{Ca}^{B} as

$$I_{\text{ps}} = \frac{w}{1 + \exp[-(|I_{\text{Ca}}^{\text{B}}| - \theta)/\epsilon]}, \quad (16)$$

where I_{Ca}^{B} is given by Eq. A10, w is the strength of synaptic connection, θ is the threshold value of $|I_{\text{Ca}}^{\text{B}}|$ for the transmitter release, and ϵ is the parameter determining the rising of the sigmoid curve. We represent I_{ps} as a function of $|I_{\text{Ca}}^{\text{B}}|$, because I_{Ca}^{B} has a negative value due to the definition of the positive direction of I_{B} , as shown in Fig. 2.

Expression of electrical stimulus

We express the external stimulus I_{stim} to the receptor system as a function of time t . We consider the case in which the jamming signal is made by mixing of the EOD current of a relevant fish with the current of one neighboring fish. Because the EOD current is approximately represented as a sine wave (Heiligenberg, 1986), we present the stimulus current as

$$I_{\text{stim}}(t) = I_1 \sin(2\pi f_1 t) + I_2 \sin(2\pi f_2 t + \alpha), \quad (17)$$

where I_1 and f_1 are the amplitude and the frequency of EOD current for the relevant fish, respectively; I_2 and f_2 are those for its neighbor; and α is the phase shift. The magnitude of I_2 is decreased as the distance between the relevant fish and its neighbor is increased, although the magnitude of I_1 is constant.

Preparation for numerical calculations

We adopted the values listed in Table 1 for the quantities used in the present model. We describe briefly the reasons why we adopted the values.

The ratio of S_{A} and S_{B} comes from the observed results (Wachtel and Szamier, 1966) that about 95% of the surface membrane of the receptor cell is exposed to the lumen and the remaining 5% of the cell surface corresponds to the basal membrane. We consider roughly that the area S_{T} of the tight junctions between the receptor cell and its supporting cell is comparable with the area S_{B} of the basal membrane, because the calculated results are not sensitive to values of $S_{\text{T}}/S_{\text{B}}$. The values of C_{Na}^{C} , C_{K}^{C} , and C_{Ca}^{C} were taken as typical values in an intracellular region, and the values of C_{ν}^{I} ($\nu = \text{Na}^+, \text{K}^+, \text{Ca}^{2+}$) were also adopted as typical values in a serosal bath. The values of C_{ν}^{L} correspond to the values in the 10% marine water. The anion concentrations C_{Cl}^{Y} ($\text{Y} = \text{L}, \text{C}, \text{I}$) are obtained from the charge neutrality as

$$C_{\text{Cl}}^{\text{Y}} = C_{\text{Na}}^{\text{Y}} + C_{\text{K}}^{\text{Y}} + 2C_{\text{Ca}}^{\text{Y}}. \quad (18)$$

Because the ion permeabilities P_{ν}^{X} of leak channels have not been measured yet for the electroreceptor organs, we estimated very roughly that their values are on the order of 10^{-11} m/s (Fidelman and Mierson, 1989) and $P_{\text{Na}}^{\text{T}} = P_{\text{K}}^{\text{T}} = P_{\text{Cl}}^{\text{T}}$. The values of P_{ν}^{A} were changed around the values of 5×10^{-11} m/s, so as to obtain a reasonable value for the membrane potential ϕ_{A} in the resting state. It is noted that the essential feature of response properties of the receptor cell system is quite insensitive to the values of P_{ν}^{A} and P_{ν}^{T} . The values of P_{ν}^{B} were adjusted so that the damped receptor oscillations might occur in the T-receptor systems.

The values of the parameters appearing in the conductivity g_{Ca}^{B} (Eqs. A1–A4) are the same as the relevant values determined for hair cells by Hudspeth and Lewis (1988a), except for the value of g_{Ca}^{B} . The values of the parameters used in $g_{\text{K(Ca)}}^{\text{B}}$ (Eqs. A5–A8) are the same as the relevant values determined by Hudspeth and Lewis (1988a), except

TABLE 1 The standard values of the physical quantities included in the model and the equations relevant to the definition of the quantities

Quantity	Definition (Eq.)	Value
S_X	1, 2	$S_B = \text{unity}, S_A = 20 S_B, S_T = S_B$
C_X	3–5	0.01 F/m ² for $X = A, B, T$
T	6	298.5 K
C_ν^L	6	$C_{Na}^L = 15.0, C_K^L = 0.0, C_{Ca}^L = 0.0$ (mM)
C_ν^C	6	$C_{Na}^C = 5.0, C_K^C = 150.0, C_{Ca}^C = 0.01$ (mM)
C_ν^I	6	$C_{Na}^I = 150.0, C_K^I = 5.0, C_{Ca}^I = 1.0$ (mM)
P_ν^A	14	1.0, 9.8, 0.5 ($\times 10^{-11}$ m/s) for $\nu = Na^+, K^+, Cl^-$
P_ν^B	14	2.0, 5.0, 1.0 ($\times 10^{-9}$ m/s) for $\nu = Na^+, K^+, Cl^-$
P_ν^T	14	5.0, 5.0, 5.0 ($\times 10^{-11}$ m/s) for $\nu = Na^+, K^+, Cl^-$
C_N	15	0.01 F/m ²
\bar{g}_{Na}	15	1200 S/m ²
\bar{g}_K	15	400 S/m ²
\bar{g}_L	15	2.4 S/m ²
V_{Na}	15	56.0 mV
V_K	15	-93.0 mV
V_{Cl}	15	-30.0 mV
w	16	4.7
θ	16	150 mA/m ²
ϵ	16	50 mA/m ²
α	17	π
\bar{g}_{Ca}^B	A1	300 S/m ² for T-receptor; 15 S/m ² for P-receptor
α_0	A3	22800 s ⁻¹
V_A	A3	8.01 mV
K_A	A3	510 s ⁻¹
V_0	A3, A4	70.0 mV
β_0	A4	0.97 s ⁻¹
V_B	A4	6.17 mV
K_B	A4	940 s ⁻¹
k_{-j}	A5	6, 100, 30 ($\times 10^3$ s ⁻¹) for $j = 1-3$
β_C	A5	1000 s ⁻¹
$\bar{g}_{K(Ca)}^B$	A6	250 S/m ² for T-receptor; 500 S/m ² for P-receptor
δ_j	A7	0.2, 0, 0.2 for $j = 1-3$
$K_j(0)$	A7	6, 45, 20 (μ M) for $j = 1-3$
V_α	A8	33 mV
$\alpha_C(0)$	A8	450 s ⁻¹
K_S	A9	28000 s ⁻¹
U	A9	0.2
ξ	A9	3.4×10^{-6}
l	A9	25 μ m
$\beta_h(\infty)$	A15	$1.8 (10^{-3} \text{ s})^{-1}$

for the values of $\bar{g}_{K(Ca)}^B$ and k_{-j} ($j = 1-3$). We modified the values of \bar{g}_{Ca}^B and $\bar{g}_{K(Ca)}^B$ for T-receptor systems so that the model of the T-receptor could signal correctly the zero crossing time of the stimulation current I_{stim} , and we modified the values for P-receptor systems so that the P-receptor model could code variations in amplitude of I_{stim} . The values of k_{-j} ($j = 1-3$) were adjusted so as to reproduce the observed value of the optimum frequency of T-units.

The values of the parameters in Eq. A9 are the same as the relevant values determined for hair cells by Hudspeth and Lewis (1988a), except for the values of U , ξ , and K_S . They were adjusted so that the damped receptor oscillations might occur in the T-receptor systems.

The values of parameters used in the Hodgkin-Huxley equations (Eq. 15 and Eqs. A11–A16) are the same as the relevant values used by Hodgkin and Huxley (1952), except

for $\beta_h(\infty)$. We modified the values of $\beta_h(\infty)$ so that the afferent nerve could become responsive to the stimulation current I_{stim} with high frequency (~ 600 Hz).

The values of parameters w , θ , and ϵ in Eq. 16 were adjusted so that the afferent nerve could generate impulses while maintaining both the function of T-receptor system as a phase encoder and that of P-receptor system as an amplitude encoder.

RESULTS AND DISCUSSION

The two kinds of receptor systems, P-receptors and T-receptors, have several quite different properties. P-receptors respond primarily to changes in the amplitude of the stimulus, and have high thresholds of stimulus intensity for firing of a single spike during each stimulus cycle, broad tuning curves with respect to stimulus frequencies, and long latencies of response. T-receptors fire one spike for every cycle of stimulus with a very constant phase, and have low thresholds, sharp tuning curves, and short latencies.

In the present section, we show that the functional differences between P- and T-receptors come mainly from the difference in relative strength of contributions of voltage-sensitive Ca^{2+} channels and Ca^{2+} -activated K^+ channels to the response function of P- and T-receptors. The relative strength of contributions of these channels depends linearly on the densities and ionic conductances of these channels in the receptors. In the following subsections, we describe the functional differences between P- and T-receptors based on the difference in the density. We can also obtain the equivalent results based on the difference in the conductance of a single ion channel, because the single channel conductance as well as the channel density contribute linearly to electric current across the basal membrane.

Furthermore, we show that many fundamental properties of the receptors are systematically reproduced by using the present model, and microscopic origins of the properties are clarified based on the calculated results.

Response patterns to jamming signals

We calculated the temporal variations in the membrane potentials of the receptor cells and in the impulsive responses of the afferent nerve fiber, which were induced by various kinds of stimuli, given by Eq. 17. The calculated results are shown for a P-receptor and a T-receptor in Fig. 3 in the case where $I_1 = 0.7 \mu\text{A}/\text{cm}^2$, $I_2 = 0.3 \mu\text{A}/\text{cm}^2$, $f_1 = 400$ Hz, $f_2 = 405$ Hz, and the values of the other parameters are the same as those given in Table 1. The P-afferent fiber fires intermittently, and the firing rate increases with increasing amplitude of stimulus, that is, the model of the P-receptor can function as an encoder of amplitude modulation. The T-afferent fiber fires a spike on every cycle of the stimulus and in perfect phase synchrony with the stimulus, that is, the model of the T-receptor can code every positive zero crossing time of the stimulus.

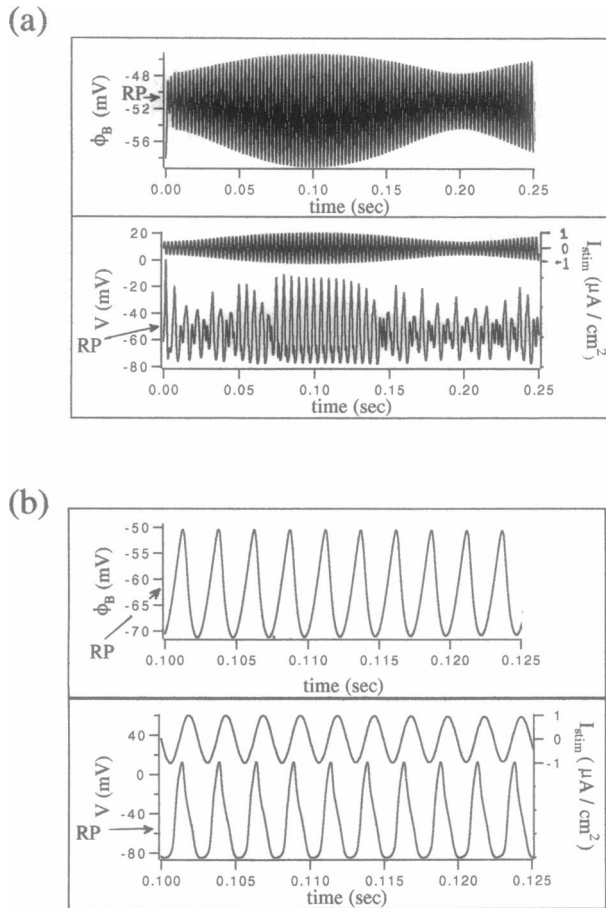


FIGURE 3 Response of membrane potentials of the receptor cell (ϕ_B , uppermost graph) and of the afferent nerve (V , lowermost graph) for (a) the P-receptor and (b) the T-receptor. A jammed stimulus (I_{stim}) is shown in the middle graph, and the parameter values for the stimulus are $I_1 = 0.7 \mu\text{A}/\text{cm}^2$, $I_2 = 0.3 \mu\text{A}/\text{cm}^2$, $f_1 = 400 \text{ Hz}$, $f_2 = 405 \text{ Hz}$. RP denotes the resting potential of the cell or the nerve. The time scale is quite different between the P- and T-receptors, to show clearly their functions as encoders of amplitude modulation and zero crossing time, respectively.

We consider what accounts for the functional difference between the two kinds of receptors. It is seen in Table 1 that the values of \bar{g}_{Ca}^B and $\bar{g}_{K(Ca)}^B$ for the T-cell are different from those for the P-cell. This means that the population density of the Ca^{2+} channels in the T-cell is 20 times as large as that in the P-cell, whereas the density of the K^+ channels in the T-cell is half the density in the P-cell. The driving force of change in the membrane potential ϕ_B under stimulation is generated by the Ca^{2+} channels, whereas the suppressing force of the change is generated by the K^+ channels. Because in the T-cell, the driving force is much stronger than the suppressing force, the potential changes in the directions both of depolarization and hyperpolarization are very large, as seen in Fig. 3 *b*. On the other hand, the potential changes in the P-cell are very small, as seen in Fig. 3 *a*, because the driving force is comparable to the suppressing force. Then, the Ca^{2+} current I_{Ca}^B of the T-cell is large enough to give a strong postsynaptic current I_{ps} , by which a spike can be generated in the T-afferent fiber (see Eqs. 15 and 16),

whereas I_{Ca}^B of the P-cell is not so large that the P-afferent fiber can fire a spike on each depolarization of the receptor cell.

The contribution of Ca^{2+} -activated K^+ channels is important essentially for the function of P-receptor. Even if the amplitude of stimuli is small and, as a result, the magnitude of I_{ps} is small, the nerve cell can fire spikes when the receptor cell is depolarized for a long time, and as a result the postsynaptic current I_{ps} flows continuously during this time. The period of depolarization of the receptor cells shortens with increasing population density of the K^+ channels. Therefore, the large density is required for the P-cell rather than for the T-cell, as seen in Table 1, so that the P-receptor becomes an amplitude encoder.

We investigated the range of the values for the main frequency f_1 , for the frequency difference $Df \equiv f_2 - f_1$, and for the intensity ratio I_2/I_1 , in which the P- and T-receptor systems, the parameter values of which are given in Table 1, work reliably as an encoder of amplitude modulation and a phase encoder, respectively. The result is shown in Table 2.

The reliability ranges are generally narrower for the P-receptor than for the T-receptor. The envelope curve of the stimulus oscillation curves becomes more complex as the values of Df and I_2/I_1 deviate from the values for which simple beat patterns are formed. The P-receptor has a greater difficulty coding the structure of the envelope curve as the structure becomes more complex. On the other hand, the detection of zero crossing points of the stimulus oscillation curves by the T-receptor is easy compared with the task of the P-receptor.

Dependence of discharge rate on stimulus intensity

We showed above that the difference in response properties between the P- and T-receptors arises mainly from the difference in the population densities of their Ca^{2+} channels. Then the P-afferent fiber should fire one spike for each cycle of the sinusoidal stimulus as the T-afferent fiber does, when the strength of stimulus is increased enough. On the other hand, the firing probability of T-afferent fiber should become less than one, like that of the P-afferent fiber in a normal condition, when the stimulus intensity is decreased enough.

The property expected for the P-receptor has been observed (Hopkins, 1976; Scheich et al., 1973). It has been

TABLE 2 The reliable ranges of the main frequency f_1 , the frequency difference $|f_2 - f_1|$, and the intensity ratio I_2/I_1 for a P-receptor and a T-receptor

Stimulus parameters	P-receptor	T-receptor
f_1 (Hz)	250–500	200–600
$ f_2 - f_1 $ (Hz)	2–20	2–40
I_2/I_1	0.36–1	0–1

The relations of a jammed stimulus to f_1 , f_2 , I_1 , and I_2 are given in Eq. 17. The parameter values used for the P- and T-receptors are given in Table 1.

found that a value of the threshold intensity for one-to-one firing depends on the frequency of stimulus. The calculated results also reproduced the property expected for the P-afferent discharge. The calculated results for the frequency dependence will be described in a later subsection on the tuning property.

The property expected for the T-afferent fiber also has been observed (Scheich et al., 1973). The number of discharges per second was measured as a function of stimulus intensity for several frequencies of stimulation (Scheich et al., 1973). There appears a plateau at half the maximum number of discharges, where the number is equivalent to the value in hertz of stimulus frequency.

We show in Fig. 4 the calculated results for the dependence of discharges of the T-afferent fiber on intensity of the stimuli whose frequency is 350 Hz and 250 Hz. The number of discharges is nearly proportional to the logarithm of stimulus intensity, except for half the maximum number of discharges. When the discharge number is near half the maximum number, the discharge number is fixed over a wide range of the intensity, that is, a plateau appears at the number.

The existence of the plateau means that a one-to-two firing pattern is more stable in the T-afferent fiber than the other patterns with rates of one to more than two. It is seen in Fig. 4 that the width of the plateau is larger for the

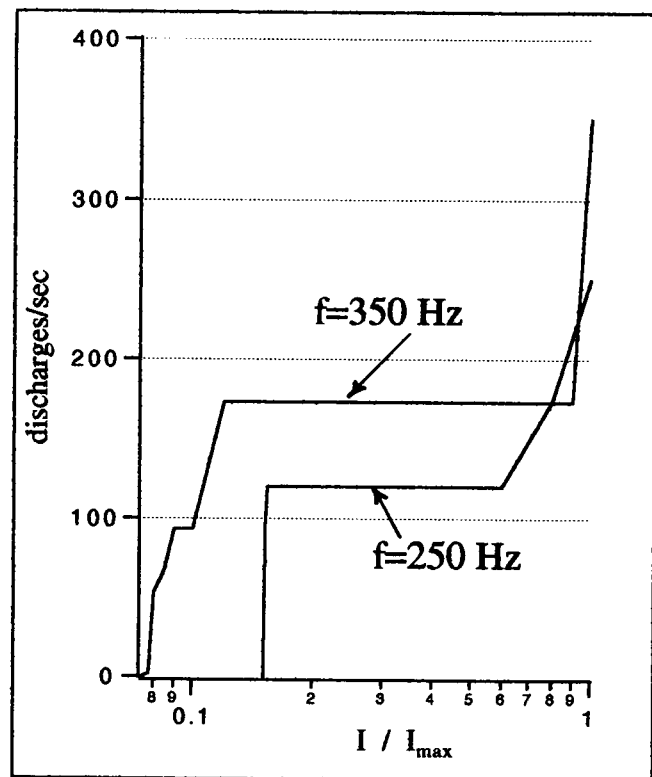


FIGURE 4 Dependencies of discharges of the T-afferent nerve on intensity I of the stimulus with sinusoidal wave whose frequency is 350 Hz or 250 Hz. I_{max} means the threshold intensity for the 1:1 firing, which is $0.18 \mu\text{A}/\text{cm}^2$ for 350 Hz and $0.25 \mu\text{A}/\text{cm}^2$ for 250 Hz.

stimulus with 350 Hz than for that with 250 Hz. Because the sensitivity of the T-receptor model used is tuned to the stimulus frequency of about 400 Hz, the stability of a one-to-two firing pattern decreases as the stimulus frequency deviates from 400 Hz.

Receptor oscillation

A damped electric oscillation has been recorded from the pore of a tuberous electroreceptor organ, when the receptors are stimulated with electric field pulses (Meyer and Zakon, 1982; Viancour, 1979b; Zakon, 1984). It has been also observed (Keller et al., 1986; Meyer et al., 1984; Zakon, 1986b) that frequencies of the underdamped receptor oscillation correspond approximately to the best frequencies of electroreceptors to which the afferent nerve fiber is most sensitive or tuned. Many workers have suggested (Bastian, 1994; Keller et al., 1986; Meyer et al., 1984; Sanchez and Zakon, 1990; Zakon, 1986b; Zakon and Meyer, 1983) that there exists a close correlation with respect to microscopic mechanism between the frequency sensitivity of the receptors and the underdamped receptor oscillation, although they have not yet clarified the mechanism through which the two properties correlate quantitatively as well as qualitatively to each others.

In the present subsection, we consider the mechanism of damped oscillations of receptor cell potentials induced by a single electric pulse stimulation, to clarify in the following subsections the microscopic origin of the differences in frequency tuning curve and in response latency between the P- and T-receptors.

The calculated damped oscillations are shown in Fig. 5, *a* and *b*, for the P- and T-receptor cells, respectively, the parameter values of which are given in Table 1. The damped oscillations may be induced by the following processes: 1) A impulsive current stimulus depolarizes the basal membrane potential ϕ_B . 2) Voltage-sensitive Ca^{2+} channels are activated by the depolarization, and the inward Ca^{2+} current I_{Ca}^B (Eq. A10) increases and accelerates the depolarization. 3) The concentration C_{Ca}^C of intracellular Ca ions increases and Ca^{2+} -activated K^+ channels are activated. 4) The outward K^+ current $I_{K(Ca)}^B$ suppresses the increase in ϕ_B , and ϕ_B begins to decrease. Then the Ca^{2+} channels are deactivated. Because I_{Ca}^B is decreased, the repolarization of ϕ_B is accelerated. ϕ_B overshoots the resting potential due to the acceleration of repolarization. 5) The K^+ channels are deactivated with decreasing C_{Ca}^C . Because $I_{K(Ca)}^B$ is decreased, the decrease in ϕ_B is suppressed, and ϕ_B begins to increase. 6) The Ca^{2+} channels are activated again and accelerate the increase in ϕ_B . ϕ_B overshoots the resting potential, and process 2 occurs again.

The potential oscillation is induced by the regular cycles of Ca^{2+} channel activation \rightarrow K^+ channel activation \rightarrow Ca^{2+} channel deactivation \rightarrow K^+ channel deactivation. An effect of the cycles appears clearly on the variation in the intracellular Ca^{2+} concentration C_{Ca}^C . We show the variation in C_{Ca}^C during damped oscillation in Fig. 5.

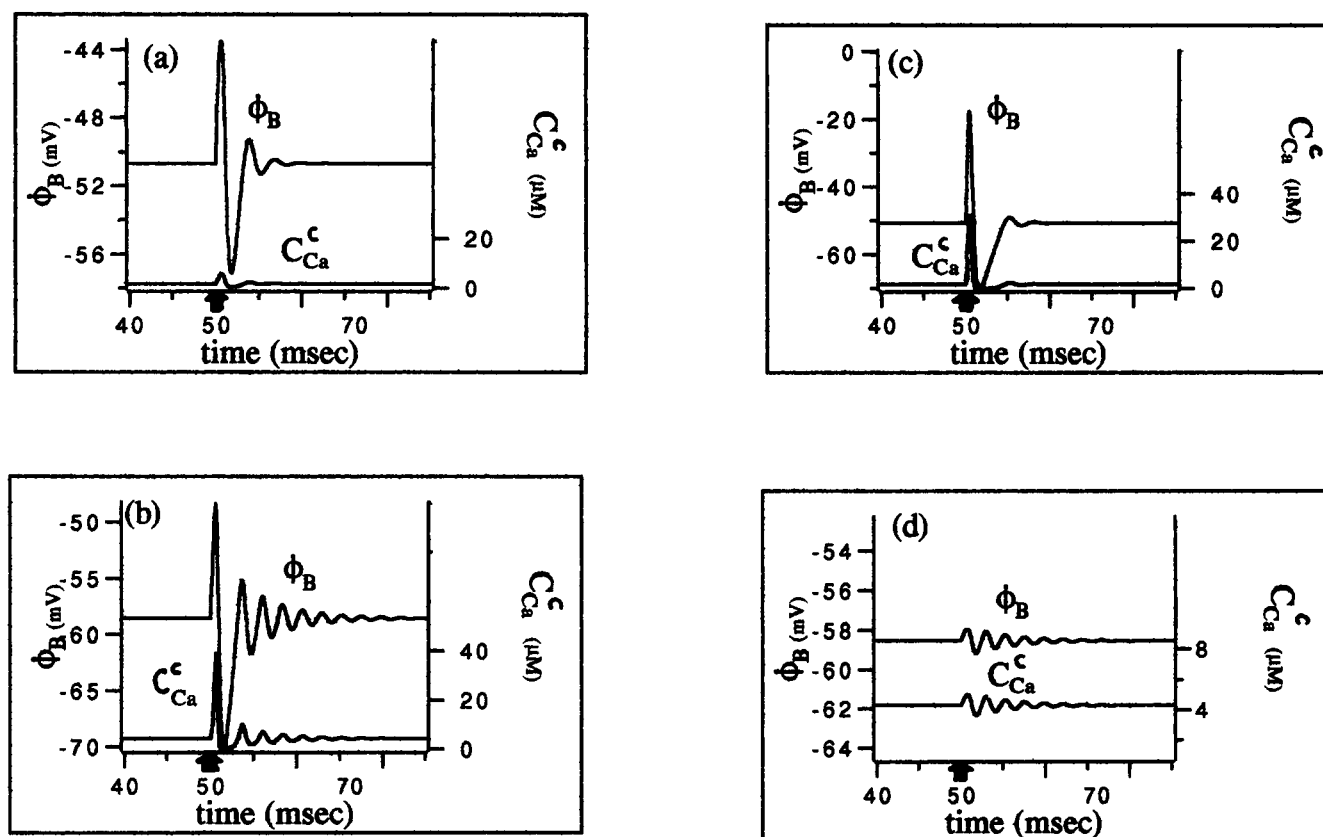


FIGURE 5 Damped potential oscillations (receptor oscillations) ϕ_B of the receptor cell induced by a single pulse current with height of I_p and width of 1 ms, and the variation of intracellular Ca^{2+} concentration C_{Ca}^c . (a) for P-receptor with $I_p = 1.5 \mu\text{A}/\text{cm}^2$, (b) for T-receptor with $I_p = 1.5 \mu\text{A}/\text{cm}^2$, (c) for P-receptor with $I_p = 10.0 \mu\text{A}/\text{cm}^2$, and (d) for T-receptor with $I_p = 0.15 \mu\text{A}/\text{cm}^2$. The pulse current is applied at the time denoted by an arrow.

The direct contributions of the Ca^{2+} channels and the Ca^{2+} -activated K^+ channels to the damped oscillations have been confirmed experimentally (Zakon, 1984). The oscillation is suppressed by blockers of Ca^{2+} channels and by blockers of K^+ channels.

The frequency and number of the damped oscillation for the P-receptor cell are noticeably different from those for the T-receptor cell, as seen in Fig. 5. Because the difference in the tuning property between P- and T-receptors arises from the difference in the damped oscillation, as will be shown in the next subsection, we describe briefly below the origin of the differences.

The difference in the damped oscillation patterns arises from the difference in the relative strength of the driving force generated by the Ca^{2+} channels and the suppressing force generated by the K^+ channels. Because the driving force of potential change overwhelms the suppressing force in the T-cell, the potential of the cell may be changed quickly and sensitively by a small deviation from the resting state. Therefore, the frequency and number of the oscillation become large. On the other hand, the driving force is comparable to the suppressing one in the P-cell, and as a result the potential deviation from the resting potential is slowly restored but well damped. Therefore, the frequency and number of cycles of the oscillation become small.

It may be expected from the origin producing the difference that the pattern of damped oscillation does not change, depending on the intensity of an impulsive stimulus. The calculated pattern for the P-receptor cell is shown in Fig. 5 c in the case where the stimulus intensity is seven times as strong as that used in Fig. 5 a. The calculated pattern for the T-cell is shown in Fig. 5 d, where the intensity is one-tenth the intensity used in Fig. 5 b. It is seen from the calculated results that the underdamped oscillation pattern is quite insensitive to the stimulus intensity, although amplitudes of the oscillation depend on the intensity.

Frequency dependence of threshold intensity

The threshold intensity of sine wave stimulation, at which the criterion for firing of a spike per the stimulation cycle is satisfied, depends on the frequency of the stimulation (Hopkins, 1976; Viancour, 1979a). The curve of the threshold intensity versus the frequency becomes roughly a V shape for the T-receptor, that is, an optimum frequency exists at which the threshold intensity becomes a minimum. On the other hand, the curve for the P-receptor has no noticeable minimum. Values of the threshold intensity are noticeably higher for the P-receptor than for the T-receptor.

We calculated the threshold intensity for the P- and T-receptors as a function of stimulus frequency. The result is shown in Fig. 6. The calculated curves are quite similar to the curves observed for *Eigenmannia* (Hopkins, 1976).

To clarify the microscopic reason why the T-receptor has the frequency to which the T-afferent fiber is most sensitive and the P-receptor does not have an optimum frequency, we consider the role of damped receptor oscillations in the response of receptor cell to sine wave stimuli. We show in Fig. 7 the calculated variations in the membrane potential of receptor cells induced by the stimuli with a common amplitude but with different frequencies. The damped receptor oscillation induced by a pulse stimulus is also shown in the relevant figure.

The magnitude of depolarization of the T-receptor cell becomes a maximum, as seen in Fig. 7 b, when the potential oscillation induced by a sine wave stimulus is resonant with the inherent potential oscillation of the cell originating from the damped receptor oscillation. Because the cell is stimulated every cycle by the external stimulus, the inherent oscillation is not damped under the resonance condition, and as a result contributes to the responsive depolarization of the cell. Therefore, the optimum frequency corresponds to the frequency of damped receptor oscillation.

On the other hand, the depolarization of the P-receptor cell does not become a maximum for the stimulus whose

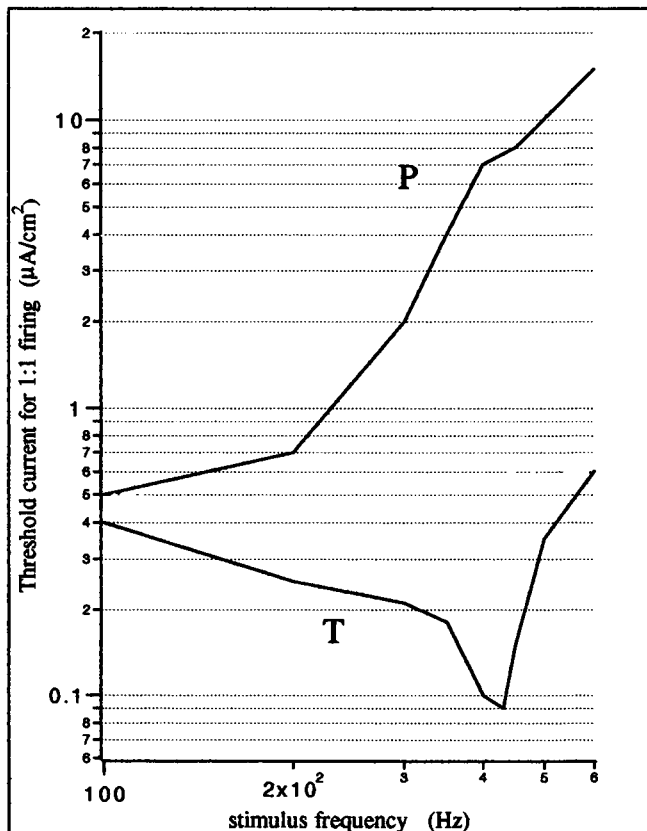


FIGURE 6 Dependence of the threshold intensity of sine wave stimulation for the 1:1 firing on the stimulus frequency in the P- and T-receptors.

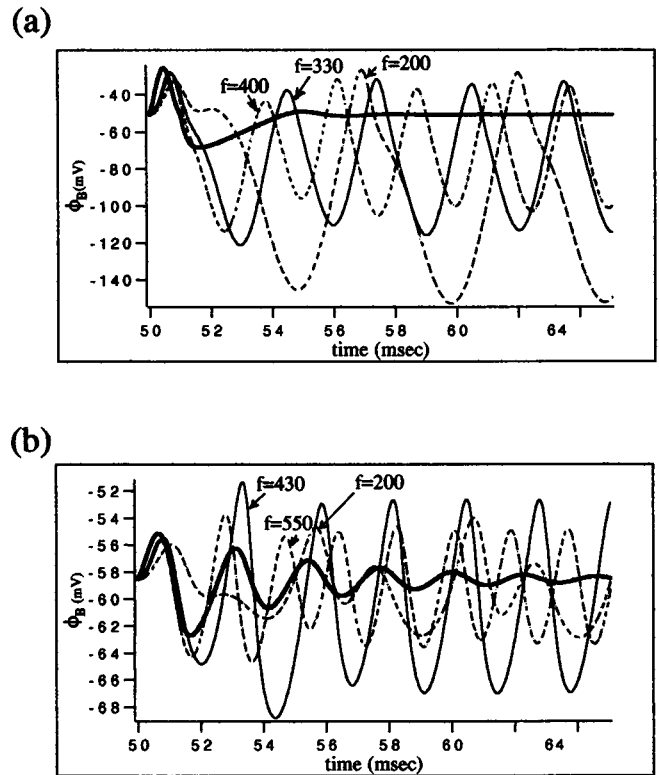


FIGURE 7 Variations in the potential ϕ_B of the receptor cell induced by the sine wave currents with a common intensity ($7.0 \mu A/cm^2$ for P-receptor and $0.6 \mu A/cm^2$ for T-receptor) but with different frequencies f denoted on each line (a) for the P-receptor and (b) for the T-receptor. The damped receptor oscillation included by a pulse current, the intensity of which is equivalent to that of the sine wave currents, is also shown by a heavy line, to show how a resonance can occur between a stimulus oscillation and the receptor oscillation.

frequency is equivalent to the frequency (330 Hz) of the receptor oscillation, as seen in Fig. 7 a. This comes from the two properties of the P-cell. The cell requires a large stimulus intensity for the 1:1 firing. The magnitude of depolarization at the second peak of the damped receptor oscillation becomes negligibly small compared with the depolarization at the first peak with increasing the stimulus intensity, as seen from Fig. 5, a and c. Therefore, the contribution of the receptor oscillation to the responsive depolarization of the P-cell is negligible, as seen in Fig. 7 a.

Stimulus dependence of spike latency

A period of spike latency, which is usually defined as a period from the positive zero crossing time of the stimulus to a spike generation time of the afferent nerve, is much longer for the P-receptor than for the T-receptor (Scheich et al., 1973). The spike latency for the T-receptors is shortened as the stimulus intensity is increased (Scheich et al., 1973).

This comes from the fact that the period from an injection of postsynaptic current I_{ps} to a spike generation in nerve axons depends on the magnitude of I_{ps} , that is, the period is shortened with increasing I_{ps} (Hodgkin and Huxley, 1952).

The magnitude of I_{ps} depends on the magnitude of depolarization of receptor cells. Because the magnitude of depolarization induced by a common stimulus is much larger for the T-receptor than for the P-receptor, as seen in Fig. 3, the latency in the T-receptor becomes much shorter than that in the P-receptor. When a magnitude of stimulation is changed, the latency decreases with increasing magnitude.

Bastian and Heiligenberg (1980) found from the response of the T-receptor to mixed stimuli (Eq. 17) consisting of two sine waves that the range of spike latency (maximum minus minimum latency) decreases with a decrease in the ratio I_2/I_1 . We show in Fig. 8 the calculated dependence of the latency range of the T-receptor on $\ln(I_2/I_1)$. The calculated result is quite similar to the observed one.

The dependence arises for the following reason. The latency becomes a maximum at a node of the beat pattern of stimuli, whereas it becomes a minimum at a loop of the beat. The difference in amplitude between the node and the loop decreases with a decrease in the ratio I_2/I_1 .

Dependence of response properties on densities of Ca^{2+} and K^+ channels

It is seen in the previous subsections that the differences in the response properties between the P- and T-receptors arise mainly from the differences in the population densities of the voltage-sensitive Ca^{2+} channels and of the Ca^{2+} -activated K^+ channels between the two receptors.

It has been observed (Hopkins, 1976; Sanchez and Zakon, 1990; Viancour, 1979a, b; Zakon, 1986b) that tuning of the threshold intensity to the optimum frequency and/or the

spike latency is changed, depending on the species of electric fish and/or ages of the fishes. Because the density of the Ca^{2+} channels and/or that of the K^+ channels seem to change, depending on the species and/or the age, we consider how the response properties of the T-receptors, the damped receptor oscillations, the tuning curves, and the spike latency are changed with the densities.

Figure 9 shows the calculated result for the frequency and number of the damped receptor oscillations as functions of $\bar{g}_{\text{Ca}}^{\text{B}}$ and of $\bar{g}_{\text{K}(\text{Ca})}^{\text{B}}$, which are proportional to the densities of the Ca^{2+} channels and of the K^+ channels, respectively. Both the frequency and the number increase with an increase in the density of the Ca^{2+} channels. The frequency increases with an increase in the K^+ channel density, but the number decreases, as seen in Fig. 9 b. Therefore, K^+ channels destabilize the receptor oscillation.

Figure 10 shows the calculated dependence of the tuning curves on the densities of the Ca^{2+} channels and of the K^+ channels. The optimum frequency increases with increasing Ca^{2+} channel density as the receptor oscillation frequency. The tuning curves are sharpened and the minimum threshold intensity is lowered as the Ca^{2+} channel density is increased. On the other hand, the variation of the tuning curves with the K^+ channel density is complex, as seen in Fig. 10, because the frequency of receptor oscillation increases with the density but the receptor oscillation is destabilized. Therefore, the curve (f) does not have a clear optimum frequency.

Viancour (1979b) showed that the latency difference relates, roughly speaking, linearly to half the period of individual fish EODs, where the latency difference means the difference in latency between the first spike induced by an impulsive inward current (positive stimulation) and that by an impulsive outward current (negative stimulation). It was also shown (Viancour, 1979b) that the magnitude of the difference is independent both of the stimulus intensity and duration. We calculated a dependence of the latency difference on half the reciprocal of optimum frequency by changing the densities of the Ca^{2+} channels and the K^+ channels. The result is shown in Fig. 11, where the latency for the impulsive inward current is defined as time period from initiation of the current to the first spike, but the latency for the impulsive outward current is defined as a period from termination of the current to the first spike. Then the dependence is roughly linear and the latency difference is independent of both the intensity and duration of pulse stimuli. Because the frequency of EOD is approximately equal to the optimum frequency (Hopkins, 1976; Hopkins and Heiligenberg, 1978; Scheich et al., 1973; Viancour, 1979a; Zakon, 1986b; Zakon and Meyer, 1983), the reason from which the roughly linear relationship observed arises is qualitatively equivalent to the reason why the latency difference depends linearly on half of the reciprocal of the optimum frequency.

Essentially, the reason is based on the fact that the first spike generated by an inward pulse current is just the nerve response induced by the first depolarization peak of the

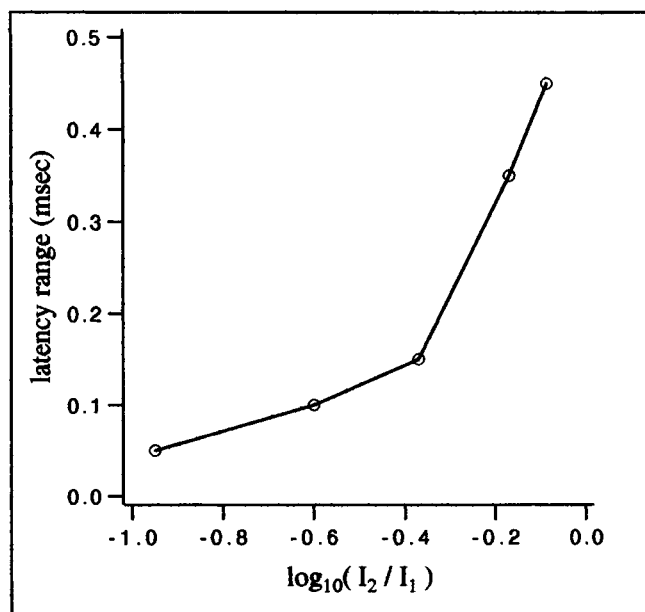


FIGURE 8 Dependence of the range of spike latency in the response of T-receptor to jammed stimuli I_{stim} on the ratio I_2/I_1 . The range means maximum latency minus minimum latency. The values relevant to the stimuli are $I_1 = 0.7 \mu\text{A}/\text{cm}^2$, $f_1 = 400 \text{ Hz}$, and $f_2 = 405 \text{ Hz}$.

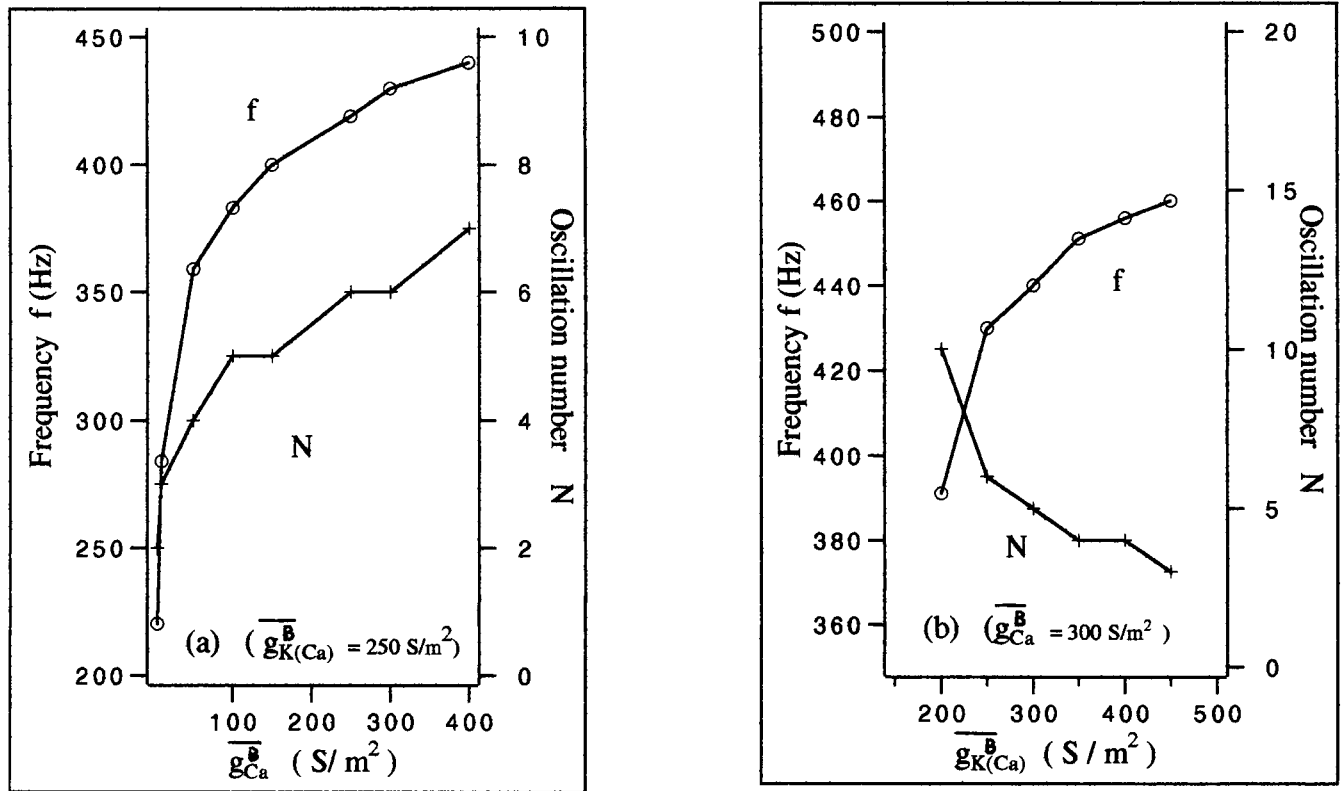


FIGURE 9 Dependencies of the frequency f and number of cycles of oscillation N of underdamped receptor oscillations on the population density (a) of voltage-sensitive Ca^{2+} channels and (b) of Ca^{2+} -activated K^+ channels. Because the population density is proportional to the maximum conductivity \bar{g}_v^B for the relevant channels, values of \bar{g}_{Ca}^B and $\bar{g}_{K(Ca)}^B$ are plotted on the abscissa in a and b, respectively. Every receptor oscillation is induced by a pulse current with $I_p = 1.5 \mu A/cm^2$ and a width of 1 ms.

receptor oscillation initiated by the current, whereas the first spike generated by an outward pulse current correlates closely with the second depolarization peak of the oscillation. The second peak is made as a reaction of the receptor cell to its deep hyperpolarization, as seen in Fig. 5. The outward pulse current hyperpolarizes the cell potential, and after termination of the current, the potential recovers, overshoots the resting level, and takes a depolarization peak.

The first spike generated by the outward current is equivalent, with respect to the mechanism of generation, to the spike generated by the second depolarization peak of the receptor oscillation induced by the relevant inward current. Then the latency difference is roughly equal to half the period of the receptor oscillation. Therefore, the latency difference is roughly equal to half the reciprocal of the optimum frequency and independent of both the stimulus intensity and duration.

CONCLUDING REMARKS

To obtain the microscopic basis of a better understanding of the relations among the optimum frequency, EOD frequency, and receptor oscillation frequency, several experiments have been devised. New electroreceptor organs were induced to form in regenerating cheek skin, and their tuning

properties were compared with those of intact receptors from the same fish (Zakon, 1986b). At 3 weeks after the onset of regeneration, new receptors of a given fish were broadly tuned with optimum frequencies lower than the optimum frequencies of their own intact receptors. As regenerating receptors mature, they gradually become more sharply tuned and tuned to progressively higher frequencies, until they reach the correct optimum frequency. Receptor oscillations were also recorded during the process of regeneration. Oscillations of more than 1 cycle were recorded from regenerated skin at more than 3 weeks. Frequencies of the damped receptor oscillations were increased with increasing postoperative interval.

Zakon (1986b) suggested two possible mechanisms for the gradual variations in response properties of newly generated receptor cells: 1) maturation of active membrane properties by insertion or modification of ion channels in the basal membrane of the receptor cell, and 2) changes in the passive properties of the receptor cell membrane.

It is concluded from the present theoretical study that the first mechanism is really responsible for the observed variations, but the second mechanism does not directly induce the variations. As the population density of voltage-sensitive Ca^{2+} channels in the basal membrane is increased, the frequency of the receptor oscillation and the optimum fre-

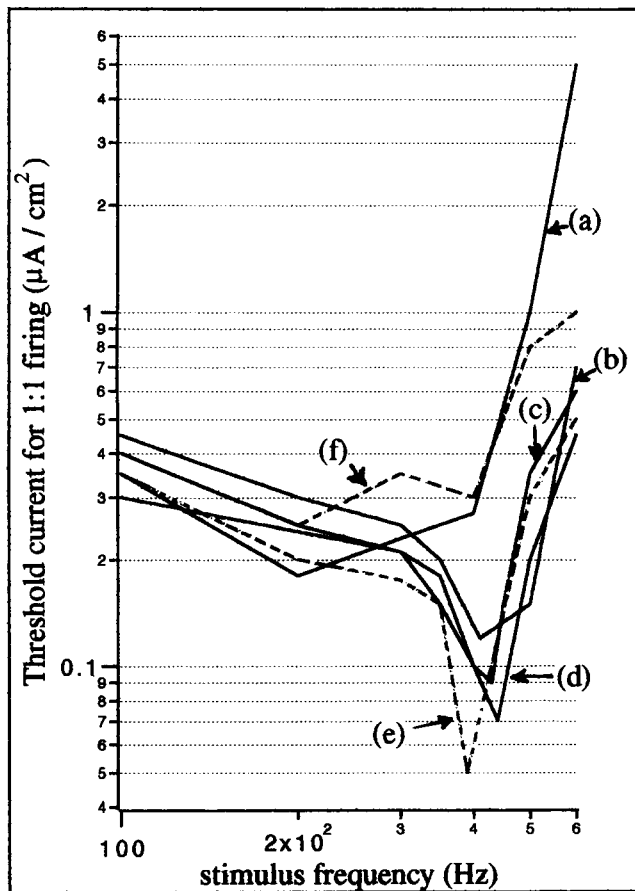


FIGURE 10 Dependence of the tuning curve on the population densities of the voltage-sensitive Ca^{2+} channels and of the Ca^{2+} -activated K^+ channels. The densities are denoted by the maximum conductivity \bar{g}^B . The values of \bar{g}_{Ca}^B , $\bar{g}_{\text{K}(\text{Ca})}^B$ in units of S/m^2 are 100, 250 for a; 200, 250 for b; 300, 250 for c; 400, 250 for d; 300, 200 for e; and 300, 350 for f.

quency are increased, and tuning to the optimum frequency becomes sharper, as seen in Figs. 9 and 10. To investigate how the receptor oscillation depends on passive properties of the receptor cells, we calculated frequencies and numbers of the receptor oscillations as functions of densities of leak channels in the apical membranes and in the tight junction, and as a function of the area ratio r_A of the apical and basal membranes. The calculated results show that the frequencies and the numbers are quite insensitive to the passive membrane properties considered, and as a result the optimum frequency does not depend on the passive properties mentioned.

Effects of steroid hormones upon electroreceptor tuning have been studied (Zakon and Meyer, 1983; Meyer et al., 1984; Keller et al., 1986). Frequencies of the receptor oscillations and the optimum frequencies were lowered in the fish injected with the hormones. It has been suggested, based on these studies, that the hormones alter the relevant characteristics of the receptor cell membranes, including the numbers of relevant ion channels. If the density of voltage-sensitive Ca^{2+} channels in the basal membrane is decreased with injection of the hormones,

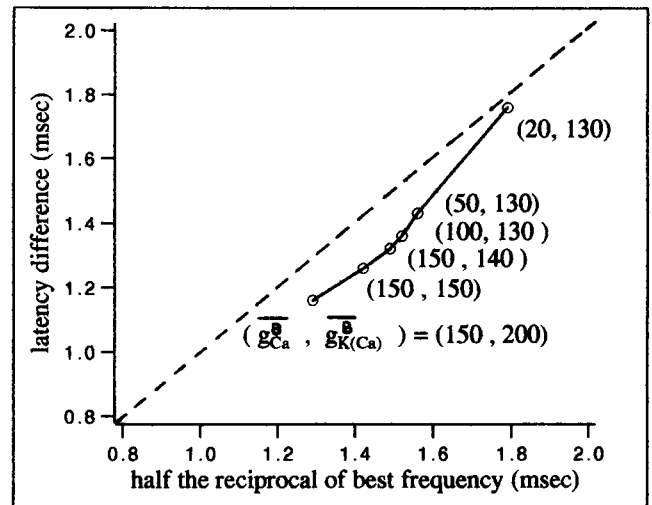


FIGURE 11 Relation of the latency difference to half the reciprocal of the optimum frequency. The latency difference means the time difference between the spike latency induced by an inward pulse current and that by an outward pulse current. The figure attached to each point denotes the values of \bar{g}_{Ca}^B and $\bar{g}_{\text{K}(\text{Ca})}^B$ (S/m^2) used to obtain the value of the optimum frequency relevant to the point. The dashed line denotes latency difference, equal to half the reciprocal of the optimum frequency.

the observed effect upon the receptor oscillation frequencies and the optimum frequencies is well expected, based on the present study.

When one compares the response properties of the present model of electroreceptor units with the relevant properties observed, one must take into account a few essential differences between the model and the real receptor units: 1) A single receptor organ includes many receptor cells (Bennet and Obara, 1986), whereas the model organ includes only one receptor cell. 2) An electroreceptive afferent fiber for the T-receptor units innervates a cluster of receptor organs (Sanchez and Zakon, 1990), whereas the afferent fiber of the present model innervates only one receptor organ. Observed responses of the afferent fiber are made by an integration of responses of many receptor cells from one or more electroreceptor organs. For example, the calculated dependence of the afferent fiber discharge on stimulus intensity shown in Fig. 4 has a very wide plateau compared with the observed plateau (figure 2 in Scheich et al., 1973).

Therefore, the response properties derived from the present model should be compared only qualitatively with the relevant properties observed, to clarify the microscopic mechanisms producing the response properties.

The integration of responses of various kinds of receptor cells is quite important for the P- and T-receptor units to encode the modulations of amplitude and phase, respectively, of stimuli under noisy conditions. The integration is a linear summation for the P-units and a nonlinear synchronization of pulse trains for the T-units. The details will be presented in a forthcoming paper.

APPENDIX

Mathematical expressions of g_{Ca}^B and $g_{K(Ca)}^B$

The conductivity of g_{Ca}^B of active Ca^{2+} channels is described by a third-order kinetic scheme of the Hodgkin-Huxley model (1952) as

$$g_{Ca}^B = \bar{g}_{Ca}^B m_c^3, \quad (A1)$$

where \bar{g}_{Ca}^B is the maximum value of the conductance when all of the channels are opened, and m_c is the gating parameter. The gating parameter m_c is given by

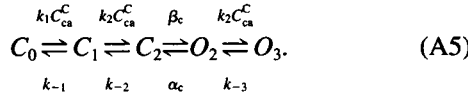
$$\frac{dm_c}{dt} = \beta(1 - m_c) - \alpha m_c, \quad (A2)$$

$$\alpha = \alpha_0 \exp[-(\phi_B + V_0)/V_A] + K_A, \quad (A3)$$

$$\beta = \beta_0 \exp[(\phi_B + V_0)/V_B] + K_B, \quad (A4)$$

where α_0 , K_A , β_0 , and K_B are rate constants and V_0 , V_A , and V_B are constant parameters.

The gating of the Ca^{2+} -activated K^+ channels is described by a linear, five-state scheme:



Here C_0 , C_1 , and C_2 represent closed states with, respectively, zero, one, or two Ca^{2+} -bound states, and O_2 and O_3 are open states with, respectively, two or three Ca^{2+} bound. Because the conductance $g_{K(Ca)}^B$ is proportional to the probabilities, $[O_2]$ and $[O_3]$, that the channels are, respectively, in the open states O_2 and O_3 , $g_{K(Ca)}^B$ is represented as

$$g_{K(Ca)}^B = \bar{g}_{K(Ca)}^B ([O_2] + [O_3]), \quad (A6)$$

where $\bar{g}_{K(Ca)}^B$ is the maximum value of the conductance. The probabilities $[C_i]$ and $[O_i]$ are obtained by solving the linear rate equations (equations 17–21 in Hudspeth and Lewis, 1988b) for the reactions (A5).

The rate constants k_j ($j = 1 - 3$) and α_c are voltage dependent and given by

$$k_j = \frac{k_{-j}}{K_j(0)} \exp(-2\delta_j F \phi_B / RT), \quad (A7)$$

$$\alpha_c = \alpha_c(0) \exp(-\phi_B / V_a), \quad (A8)$$

where $K_j(0)$ is the dissociation constant at zero membrane potential, δ_j is the fraction of the electric field experienced by Ca^{2+} at the j th binding site, $\alpha_c(0)$ is the closing rate constant at zero membrane potential, and V_a is the constant parameter. The rate constants k_{-j} and β_c are adjustable parameters.

The Ca^{2+} regulation in the receptor cell consists of three basic processes. First, Ca^{2+} entering the cell binds immediately to an excess of low-affinity intracellular buffers such that a constant fraction, U , of total Ca^{2+} remains free at any given time. Second, the binding of Ca^{2+} slows its diffusion away from the basal membrane, so that Ca^{2+} accumulates next to the membrane in small fractions, ξ , of the cell total volume, C_{vol} . Third, Ca^{2+} leaves this submembrane compartment at a rate proportional to its free concentration; the rate constant for this process is K_S . Assuming that the cell is a cylinder of diameter $2r$ and length l , the equation of Ca^{2+} concentration C_{Ca}^C in the submembrane compartment is given by

$$\begin{aligned} \frac{dC_{Ca}^C}{dt} &= \frac{US_B I_{Ca}^B}{2\xi C_{vol} F} - K_S C_{Ca}^C \\ &= \frac{U I_{Ca}^B}{2\xi l F} - K_S C_{Ca}^C, \end{aligned} \quad (A9)$$

where $S_B = \pi r^2$, $C_{vol} = \pi r^2 l$, and $I_{Ca}^B/(2F)$ is the number of Ca^{2+} entering the cell across the basal membrane in the unit of $\text{mol} \cdot (\text{m}^2 \text{s})^{-1}$. I_{Ca}^B is given by

$$I_{Ca}^B = \bar{g}_{Ca}^B m_c^3 (\phi_B - \phi_{Ca}^B). \quad (A10)$$

The rate equations for the gating parameters m , h , and n in Eq. 15

The rate equations have been derived by Hodgkin-Huxley (1952). Because we change slightly the value of a parameter used in the equations, we write here the equations to make sure:

$$\frac{dm}{dt} = \alpha_m - (\alpha_m + \beta_m)m, \quad (A11)$$

$$\frac{dh}{dt} = \alpha_h - (\alpha_h + \beta_h)h, \quad (A12)$$

$$\frac{dn}{dt} = \alpha_n - (\alpha_n + \beta_n)n, \quad (A13)$$

The rate constants α_μ and β_μ ($\mu = m, h, n$) depend on the axon potential V and are represented as

$$\alpha_m = -0.1 \frac{(V + 40)}{e^{-V+40/10} - 1}; \quad \beta_m = 4e^{-V+65/18}, \quad (A14)$$

$$\alpha_h = 0.07e^{-V+65/20}; \quad \beta_h = \frac{\beta_h(\infty)}{e^{-V+35/10} + 1}, \quad (A15)$$

$$\alpha_n = -0.01 \frac{V + 55}{e^{-V+55/10} - 1}; \quad \beta_n = 0.125e^{-V+65/80}, \quad (A16)$$

where the unit for values of α_μ and β_μ is $(10^{-3} \text{ s})^{-1}$, and the unit for V is mV. Although the value of $\beta_h(\infty)$ is 1 in the Hodgkin-Huxley equation, we modify the value to obtain the interspike distance observed for weakly electric fish.

REFERENCES

- Bastian, J. 1986. Electrolocation. In *Electroreception*. T. H. Bullock and W. Heiligenberg, editors. John-Wiley and Sons, New York. 577–612.
- Bastian, J. 1994. Electroreception. *Phys. Today*. 47:30–37.
- Bastian, J., and W. Heiligenberg. 1980. Neural correlates of the jamming avoidance response of *Eigenmannia*. *J. Comp. Physiol. A*. 136:135–152.
- Bennet, M. V. L. 1967. Mechanisms of electroreception. In *Lateral Line Detectors*. P. Cahn, editor. University of Indiana Press, Bloomington. 313–395.
- Bennett, M. V. L., and S. Obara. 1986. Ionic mechanisms and pharmacology of electroreceptors. In *Electroreception*. T. H. Bullock and W. Heiligenberg, editors. John-Wiley and Sons, New York. 157–179.
- Fidelman, M. L., and S. Mierson. 1989. Network thermodynamic model of rat lingual epithelium: effects of hyperosmotic NaCl. *Am. J. Physiol.* 257:G475–G487.
- Heiligenberg, W. 1986. Jamming avoidance responses. In *Electroreception*. T. H. Bullock and W. Heiligenberg, editors. John-Wiley and Sons, New York. 613–649.
- Heiligenberg, W. 1991. *Neural Nets in Electric Fish*. MIT Press, Cambridge, MA.
- Hodgkin, A. L., and A. F. Huxley. 1952. A quantitative description of membrane current and its application to conductance and excitation in nerve. *J. Physiol.* 117:500–544.
- Hopkins, C. D. 1976. Stimulus filtering and electroreception: tuberous electroreceptors in three species of gymnotoid fish. *J. Comp. Physiol. A*. 111:171–207.

- Hopkins, C. D., and W. H. Heiligenberg. 1978. Evolutionary designs for electric signals and electroreceptors in gymnotoid fishes of Surinam. *Behav. Ecol. Sociobiol.* 3:113-134.
- Hudspeth, A. J., and R. S. Lewis. 1988a. Kinetic analysis of voltage- and ion-dependent conductances in saccular hair cells of the bull-frog, *Rana catesbeiana*. *J. Physiol. (Lond.)*. 400:237-274.
- Hudspeth, A. J., and R. S. Lewis. 1988b. A model of electrical resonance and frequency tuning in saccular hair cells of the bull-frog, *Rana catesbeiana*. *J. Physiol. (Lond.)*. 400:275-297.
- Keller, C. H., H. H. Zakon, and D. Y. Sanchez. 1986. Evidence for a direct effect of androgens upon electroreceptor tuning. *J. Comp. Physiol. A.* 158:301-310.
- Lakshminarayanaiah, N. 1984. *Equations of Membrane Biophysics*. Academic Press, New York. 137-151.
- Meyer, J. H., and H. H. Zakon. 1982. Androgens alter the tuning of electroreceptors. *Science*. 217:635-637.
- Meyer, J. H., H. H. Zakon, and W. Heiligenberg. 1984. Steroid influences upon the electrosensory system of weakly electric fish: direct effects upon discharge frequencies with indirect effects upon electroreceptor tuning. *J. Comp. Physiol. A.* 154:625-631.
- Murray, M. J., and R. R. Capranica. 1973. Spike generation in the lateral line afferents of *Xenopus laevis*: evidence favoring multiple site of initiation. *J. Comp. Physiol.* 87:1-20.
- Pabst, A. 1977. Number and location of the sites of impulse generation in the lateral line afferents. *Xenopus laevis*. *J. Comp. Physiol. A.* 114:51-67.
- Sanchez, D. Y., and H. H. Zakon. 1990. The effects of postembryonic receptor cell addition on the response properties of electroreceptive afferents. *J. Neurosci.* 10:361-369.
- Scheich, H., T. H. Bullock, and R. H. Hamstra, Jr. 1973. Coding properties of two classes of afferent nerve fibers: high-frequency electroreceptors in the electric fish, *Eigenmannia*. *J. Neurophysiol.* 36:39-60.
- Viancour, T. A. 1979a. Electroreceptors of a weakly electric fish. I. Characterization of tuberous receptor organ tuning. *J. Comp. Physiol. A.* 133:317-325.
- Viancour, T. A. 1979b. Electroreceptors of a weakly electric fish. II. Individually tuned receptor oscillations. *J. Comp. Physiol. A.* 133:327-338.
- Wachtel, A. W., and R. B. Szamier. 1966. Special cutaneous receptor organs of fish: the tuberous organs of *Eigenmannia*. *J. Morphol.* 119:51-80.
- Zakon, H. H. 1984. The ionic basis of the oscillatory receptor potential of tuberous electroreceptors in *Sternopygus*. *Soc. Neurosci. Abstr.* 10:193.
- Zakon, H. H. 1986a. The electroreceptive periphery. In *Electroreception*. T. H. Bullock and W. Heiligenberg, editors. John Wiley and Sons, New York. 613-643.
- Zakon, H. H. 1986b. The emergence of tuning in newly generated tuberous electroreceptors. *J. Neurosci.* 6:3297-3308.
- Zakon, H. H., and J. H. Meyer. 1983. Plasticity of electroreceptor tuning in the weakly electric fish, *Sternopygus dariensis*. *J. Comp. Physiol. A.* 153:477-487.